Clinical SCIENCE

www.clinsci.org

Clinical Science (2010) 118, 583–592 (Printed in Great Britain) doi:10.1042/CS20090289

Countervailing vascular effects of rosiglitazone in high cardiovascular risk mice: role of oxidative stress and PRMT-1

Carmine SAVOIA*†‡, Talin EBRAHIMIAN*, Catherine A. LEMARIÉ*, Pierre PARADIS*, Marc IGLARZ*, Farhad AMIRI*, Danesh JAVESHGANI* and Ernesto L. SCHIFFRIN*§

*Lady Davis Institute for Medical Research, Sir Mortimer B. Davis-Jewish General Hospital, McGill University, Montreal, QC, Canada, †Cardiology Unit, Second Faculty of Medicine, Sant'Andrea Hospital, Sapienza University of Rome, Rome, Italy, ‡Research Center, Fatebenefratelli San Pietro Hospital, Rome, Italy, and §Department of Medicine, Sir Mortimer B. Davis-Jewish General Hospital, McGill University, Montreal, QC, Canada

ABSTRACT

In the present study, we tested the hypothesis that the PPARγ (peroxisome-proliferator-activated receptor γ) activator rosiglitazone improves vascular structure and function in aged hyperhomocysteinaemic MTHFR (methylene tetrahydrofolate reductase) gene heterozygous knockout (*mthfr*$^{+/-}$) mice fed a HCD (high-cholesterol diet), a model of high cardiovascular risk. One-year-old *mthfr*$^{+/-}$ mice were fed or not HCD (6 mg · kg^{-1} of body weight · day^{-1}) and treated or not with rosiglitazone (20 mg · kg^{-1} of body weight · day^{-1}) for 90 days and compared with wild-type mice. Endothelium-dependent relaxation of carotid arteries was significantly impaired (−40%) only in rosiglitazone-treated HCD-fed *mthfr*$^{+/-}$ mice. Carotid M/L (media-to-lumen ratio) and CSA (cross-sectional area) were increased (2-fold) in *mthfr*$^{+/-}$ mice fed or not HCD compared with wild-type mice ($P < 0.05$). Rosiglitazone reduced M/L and CSA only in *mthfr*$^{+/-}$ mice fed a normal diet. Superoxide production was increased in *mthfr*$^{+/-}$ mice fed HCD treated or not with rosiglitazone, whereas plasma nitrite was decreased by rosiglitazone in mice fed or not HCD. PRMT-1 (protein arginine methyltransferase-1), involved in synthesis of the NO (nitric oxide) synthase inhibitor ADMA (asymmetric ω-N^G,N^G-dimethylarginine), and ADMA were increased only in rosiglitazone-treated HCD-fed *mthfr*$^{+/-}$ mice. Rosiglitazone had both beneficial and deleterious vascular effects in this animal model of high cardiovascular risk: it prevented carotid remodelling, but impaired endothelial function in part through enhanced oxidative stress and increased ADMA production in mice at high cardiovascular risk.

INTRODUCTION

PPARγ (peroxisome-proliferator-activated receptor γ) belongs to a family of ligand-activated nuclear receptor and transcription factors, which have been extensively studied in adipocytes [1,2,4], where they are involved in fat cell differentiation and lipid storage. PPARγ is present as well in liver and skeletal muscle,

Key words: asymmetric ω-N^G,N^G-dimethylarginine (ADMA), atherosclerosis, endothelium, hyperhomocysteinaemia, peroxisome-proliferator-activated receptor γ (PPARγ), rosiglitazone.

Abbreviations: ADMA, asymmetric ω-N^G,N^G-dimethylarginine; CSA, cross-sectional area; DHE, dihydroethidium; HCD, high-cholesterol diet; H-Hcy, hyperhomocysteinaemia; L-NAME, N^G-nitro-L-arginine methyl ester; M/L, media-to-lumen ratio; MTHFR, methylene tetrahydrofolate reductase; NO, nitric oxide; NOS, NO synthase; eNOS, endothelial NOS; PPARγ, peroxisome-proliferator-activated receptor γ; PRMT-1, protein arginine methyltransferase-1; ROS, reactive oxygen species; TZD, thiazolidinedione.

Correspondence: Professor Ernesto L. Schiffrin (email ernesto.schiffrin@mcgill.ca).

other targets of insulin action [1–3] and modulate insulin sensitivity in all these tissues. Rosiglitazone is a high-affinity ligand for PPARγ belonging to the TZD (thiazolidinedione) or glitazone class of synthetic compounds clinically used in the treatment of Type 2 diabetes mellitus [1,4]. TZDs promote fatty acid oxidation and enhance insulin sensitivity in liver and skeletal muscle, in part, through inhibition of agents from adipose tissue that promote insulin resistance [5]. PPARγ is expressed in cardiovascular tissues, including heart, endothelium, vascular smooth muscle cells and monocytes/macrophages [1].

In vivo and *in vitro* studies have demonstrated that, independent of metabolic effects, PPARγ activators exert anti-proliferative, antioxidant and anti-inflammatory effects on the cardiovascular system and that they may be anti-atherogenic [1,4–10]. Hence, this class of drugs may represent a therapeutic tool for vascular protection and prevention of progression of atherosclerosis and cardiovascular disease. However, experimental and clinical studies have provided controversial results on the role of TZDs in the prevention of cardiovascular events in diabetic patients, who are at high cardiovascular risk [11]. H-Hcy (hyperhomocysteinaemia) is an independent risk factor for coronary, cerebral and peripheral atherosclerosis [12,13]. Cardiovascular risk associated with H-Hcy is particularly high when combined with other risk factors (i.e. diabetes mellitus, high cholesterol, hypertension). MTHFR (methylene tetrahydrofolate reductase) is a key enzyme in the remethylation cycle of homocysteine, which is converted into methionine [12]. A murine model of MTHFR deficiency, leading to increased plasma levels of homocysteine, develops atherosclerosis and vascular dysfunction when exposed to a HCD (high-cholesterol diet) [14]. This model mimics a common cause of mild H-Hcy in humans [15,16]. We hypothesized that chronic administration of rosiglitazone would improve vascular structure and function in *mthfr*-knockout mice fed HCD.

MATERIALS AND METHODS

Animal experiments

The study protocol was approved by the Animal Care Committee of the Lady Davis Institute and conducted in accordance with recommendations of the Canadian Council of Animal Care. Mice heterozygous for disruption of the *mthfr* gene presenting mild hyperhomocysteinaemia were generated at the Montreal Children's Hospital Research Institute as reported previously [14]. Heterozygous *mthfr*-deficient (*mthfr*$^{+/-}$) mice and wild-type controls were obtained by mating *mthfr*$^{+/-}$ mice with wild-type BALB/cAnNCrlBR (Charles River). Old adult female *mthfr*$^{+/-}$ ($n = 24$ divided into four groups as mentioned below) and wild-type ($n = 6$) littermate mice aged 11–12 months were studied. Homozygous mice have high mortality or delayed development and cerebellar abnormalities [14] and for this reason could not be studied. Heterozygous mice were divided into four groups (six mice per group) fed or not HCD (6 mg $\cdot$ kg^{-1} of body weight $\cdot$ day^{-1}; 12.5 g/kg cholesterol; Research Diets #D12336), and treated or not with rosiglitazone (20 mg $\cdot$ kg^{-1} of body weight $\cdot$ day^{-1}) for 90 days. Mice were killed by CO_2 asphyxiation.

Measurement of plasma cholesterol

Blood samples from the mice were collected in tubes containing EDTA. Plasma was separated by centrifugation and stored at $-80\,^{\circ}$C. Total plasma cholesterol was measured by enzymatic colorimetric method.

Evaluation of PPARγ expression

Snap-frozen aorta at the level of the coronary sinus was pulverized in lysis buffer [2 mM EDTA and 1 mM EGTA, with protease inhibitors: 1 μg/ml aprotinin, 1 μg/ml leupeptin, 1 μg/ml pepstatin, 1 mmol/l PMSF and 1 mmol/l Na_3VO_4]. Thereafter, samples were briefly sonicated and centrifuged (16000 *g*, 4 °C, 30 min). A portion (4 μg) of sample in a total incubation volume of 20 μl, as per the manufacturer's instructions, was analysed with an ELISA-based kit (Active Motif).

Study of internal carotid arteries

Internal carotid arteries (2–3 mm in length) were placed in ice-cold physiological salt solution containing (mmol/l) NaCl 120, $NaHCO_3$ 25, KCl 4.7, KH_2PO_4 1.18, $MgSO_4$ 1.18, $CaCl_2$ 2.5, EDTA 0.026 and glucose 5.5. They were mounted on two-glass microcannulae in a pressurized myograph. Endothelium-dependent relaxation was assessed by measuring the dilatory responses to acetylcholine (10^{-9}–10^{-4} mol/l) in vessels precontracted with noradrenaline (norepinephrine; 5×10^{-5} mol/l). Endothelium-independent relaxation was assessed by the dilatory response to sodium nitroprusside (10^{-8}–10^{-4} mol/l). To evaluate NO availability, the concentration–response curve to acetylcholine was determined before and after 30-min preincubation with the NOS (NO synthase) inhibitor L-NAME (N^G-nitro-L-arginine methyl ester; 10^{-4} mol/l). Vessels were deactivated by perfusion with Ca^{2+}-free physiological salt solution containing 10 mmol/l EGTA for 30 min. Lumen and media were measured at an intraluminal pressure at 60 mmHg as described previously [17].

Plasma nitrite measurement

Plasma nitrite as an index of NO production was evaluated with a colorimetric assay as previously described [18]. Duplicate samples of plasma (50 μl) were incubated with cadmium overnight at 4 °C with gentle shaking. Plasma was mixed with 0.01 % *N*-(1-naphtyl) ethylenediamine followed by mixing with 0.1 % *p*-aminobenzenesulfonamide, and total nitrite was determined by measuring absorbance at 548 nm.

Plasma ADMA (asymmetric ω-N^G,N^G-dimethylarginine) measurement

Blood samples were centrifuged at 3000 *g* for 10 min at 4 °C immediately after collection. Plasma samples were kept frozen at −80 °C until analysis. A total of 20 μl of plasma, as per the manufacturer's instructions, was analysed by an ELISA-based kit (DLD Diagnostika).

Oxidative fluorescent microtopography

The oxidative fluorescent dye DHE (dihydroethidium) was used to evaluate *in situ* production of superoxide [19]. Unfixed frozen ring segments of aorta embedded in OCT were cut into 5–10-μm-thick sections and placed on a glass slide. DHE (2×10^{-6} mol/l) was topically applied to each tissue section. Slides were incubated in a light-protected humidified chamber at 37 °C for 30 min and then coverslips were added [20]. Images were obtained with a Leica fluorescent microscope. The amount of DHE staining present in the vessel wall was quantified (Northern Eclipse program; EMPIX Imaging) and is expressed as a percentage of the DHE fluorescence per total surface area.

Western blot analysis for PRMT-1 (protein arginine methyltransferase-1)

Protein was extracted from the coronary sinus area of snap-frozen aorta as previously described [21]. Protein (100 μg) was separated by electrophoresis on a 10% polyacrylamide gel and transferred on to a nitrocellulose membrane. Non-specific binding sites were blocked with 5% skimmed milk in Tris-buffered saline solution with Tween for 1 h at 24 °C. Membranes were incubated overnight with anti-PRMT-1 polyclonal antibody (1:1000; Cell Signaling Technology). After incubation with the second antibody, the signal was revealed with chemiluminescence, visualized by autoradiography and quantified densitometrically.

In silico analysis of the *Prmt1* promoter

The mouse *Prmt1* gene was examined *in silico* using the UCSC genome bioinformatics web site ([22]; http://genome.ucsc.edu). The 52238857–52242238 bp region of chromosome 7 was analysed *in silico* using rVista to determine conserved PPARγ- and PPAR-response elements between mouse and human ([24]; http://genome.lbl.gov/vista/index.shtml/).

Data analysis

Data are presented as means ± S.E.M. Morphological data were compared by ANOVA, followed by Student–Newman–Keuls *post hoc* test. Statistical evaluation of mechanical parameters was performed by repeated-measures ANOVA. A value of $P < 0.05$ was considered statistically significant.

RESULTS

Mice with haploinsufficiency in MTHFR presenting mild hyperhomocysteinaemia [14] were treated or not with HCD with or without rosiglitazone. A wild-type littermate was used as control. Plasma cholesterol (Figure 1a) was similar in all the animals fed the normal diet and increased as expected in *mthfr*$^{+/-}$ mice fed HCD compared with wild-type mice ($P < 0.001$) and was significantly reduced after rosiglitazone treatment ($P < 0.05$ compared with *mthfr*$^{+/-}$ mice fed HCD). In *mthfr*$^{+/-}$ mice fed a normal diet, the expression level of PPARγ in aorta was similar to that in wild-type mice (Figure 1b). In *mthfr*$^{+/-}$ mice fed HCD, PPARγ expression was significantly increased compared with wild-type mice ($P < 0.05$). Rosiglitazone treatment induced a further increase in PPARγ expression in *mthfr*$^{+/-}$ mice fed HCD compared with untreated *mthfr*$^{+/-}$ mice fed HCD ($P<0.05$).

The M/L ratio (media-to-lumen ratio) of internal carotid arteries was similar in *mthfr*$^{+/-}$ mice fed normal diet compared with *mthfr*$^{+/-}$ mice fed HCD and, in both groups, M/L was significantly greater than in wild-type mice ($P < 0.001$; Figure 2). M/L ratio and media

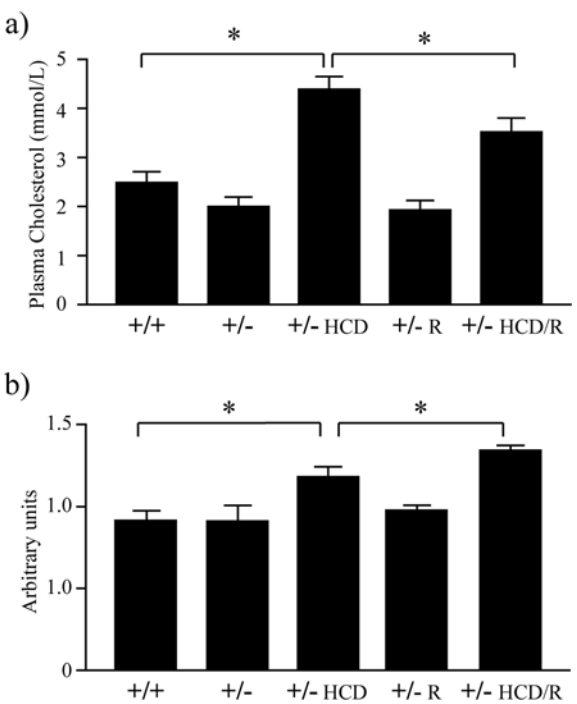

Figure 1 Plasma cholesterol (a) and PPARγ expression (b) in *mthfr*$^{+/-}$ and wild-type mice

(a) Plasma cholesterol levels in *mthfr*$^{+/-}$ and wild-type mice. (b) Expression of PPARγ at level of the coronary sinus of aorta in *mthfr*$^{+/-}$ and wild-type mice. +/+: wild-type control mice; +/—: *mthfr*$^{+/-}$ mice fed normal diet; +/— HCD: *mthfr*$^{+/-}$ mice fed HCD; +/— R: *mthfr*$^{+/-}$ mice fed normal diet and treated with rosiglitazone; +/— HCD/R: *mthfr*$^{+/-}$ mice fed HCD and treated with rosiglitazone. *$P < 0.05$.

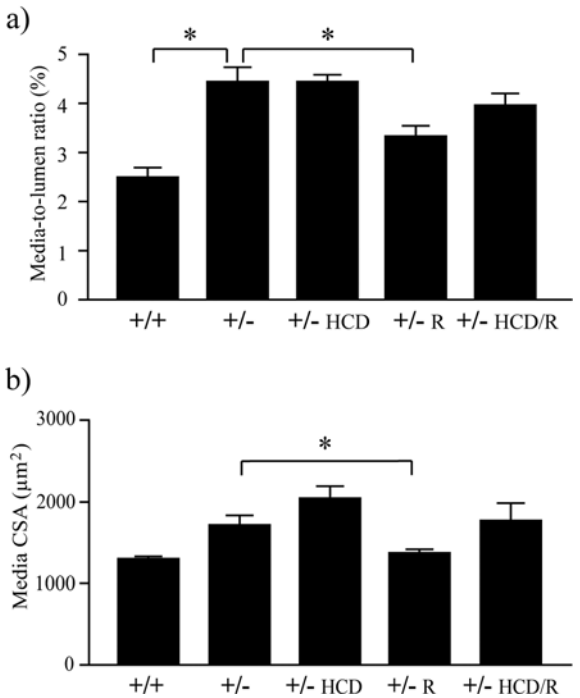

Figure 2 M/L ratio and media CSA of the carotid from *mthfr*$^{+/-}$ and wild-type mice measured at 60 mmHg intraluminal pressure

*$P < 0.05$.

CSA (cross-sectional area) were significantly smaller after rosiglitazone treatment only in *mthfr*$^{+/-}$ mice compared with untreated *mthfr*$^{+/-}$ mice when both groups were fed normal diet ($P < 0.01$ and $P < 0.05$ respectively). However, hypertrophic remodelling was not improved by rosiglitazone treatment of *mthfr*$^{+/-}$ mice fed HCD.

Endothelium-dependent relaxation of carotid arteries was similar in *mthfr*$^{+/-}$ mice fed normal diet compared with wild-type mice (Figure 3a) and was not different from *mthfr*$^{+/-}$ mice fed HCD or *mthfr*$^{+/-}$ mice fed the normal diet and treated with rosiglitazone. Vasodilation of carotid arteries in response to acetylcholine was significantly attenuated in *mthfr*$^{+/-}$ mice treated with rosiglitazone and fed HCD compared with HCD-fed *mthfr*$^{+/-}$ mice that did not receive rosiglitazone ($P < 0.05$). Endothelium-independent relaxation was similar in all groups (Figure 3b). The NOS inhibitor L-NAME significantly reduced acetylcholine-induced dilation in all groups (Figure 3c). In carotid arteries from rosiglitazone-treated *mthfr*$^{+/-}$ fed HCD, acetylcholine-induced dilation was only slightly inhibited by L-NAME (Figure 3d), indicating poor NO synthesis or bioavailability. Superoxide generation in carotid arteries was higher in *mthfr*$^{+/-}$ mice fed normal diet compared with wild-type mice ($P < 0.01$; Figure 4). A further increase was observed in *mthfr*$^{+/-}$ mice fed HCD in comparison to *mthfr*$^{+/-}$ mice fed normal diet ($P < 0.01$). Rosiglitazone did not affect superoxide production in carotid arteries of *mthfr*$^{+/-}$ mice fed the normal diet or HCD. Plasma nitrite, an index of systemic NO production, was similar in *mthfr*$^{+/-}$ mice fed the normal diet or HCD compared with the wild-type group. Rosiglitazone significantly reduced plasma nitrite concentration in both treatment groups (Figure 5a). Plasma levels of ADMA, an endogenous inhibitor of eNOS (endothelial NOS), were similar in *mthfr*$^{+/-}$ mice fed normal diet or HCD. Significantly elevated plasma ADMA levels were found in HCD-fed *mthfr*$^{+/-}$ treated with rosiglitazone ($P < 0.05$; Figure 5b). The expression of PRMT-1, a key enzyme in the synthesis of ADMA, was similar in *mthfr*$^{+/-}$ compared with wild-type mice independently of the diet. Rosiglitazone significantly enhanced PRMT-1 expression only in HCD-fed *mthfr*$^{+/-}$ (Figure 6).

The analysis of *Prmt1* gene with the UCSC genome bioinformatics web site revealed that it is contained on chromosome 7 and has four different alternative *Prmt1* mRNA splices (Figure 7b). The 52238857–52242238 bp region of chromosome 7 containing the two 5′ exons and promoter region of the *Prmt1* gene was analysed using the rVista software, and several PPARγ-response elements conserved between mouse and human were found (Figures 7a and 7c). The UCSC genome browser revealed that several regions of the *Prmt1* promoter are highly conserved among several mammalian species (Figure 7d).

DISCUSSION

Major findings from the present study of mild hyperhomocysteinaemic *mthfr*$^{+/-}$ mice demonstrate that: (i) rosiglitazone improved vascular remodelling of carotid arteries, in part by reducing plasma cholesterol levels in mice fed HCD; (ii) PPARγ agonism was associated with impaired endothelial function in the carotid arteries of *mthfr*$^{+/-}$ mice fed HCD, associated with decreased plasma nitrite and enhanced PRMT-1 expression and plasma levels of ADMA, an endogenous eNOS inhibitor; and (iii) rosiglitazone failed to reduce increased levels of ROS (reactive oxygen species) in *mthfr*$^{+/-}$ mice.

The association of several risk factors in a single individual is frequent in Western societies and contributes to the development of atherosclerosis and cardiovascular dysfunction. Age, hypercholesterolemia and H-Hcy may participate in the progression of atherosclerosis, in part by inducing oxidative stress, endothelial dysfunction and inflammation [26,27]. This is the case for the murine model of mild atherosclerosis studied here, which is characterized by advanced age, mild H-Hcy and elevated plasma cholesterol secondary to HCD. PPARγ activators exert pleiotropic effects on a wide range of tissues beyond their actions on insulin-responsive organs and tissues. These actions include

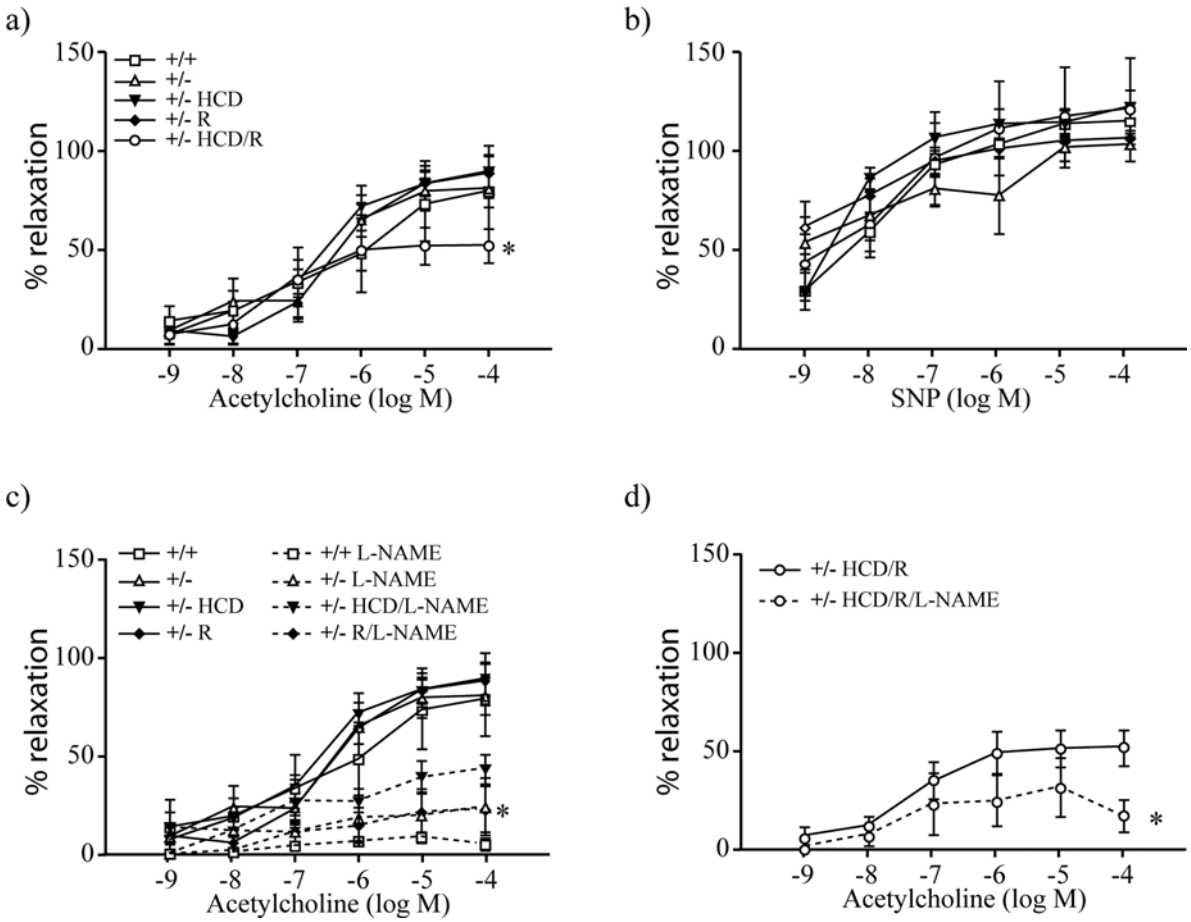

Figure 3 Concentration–response curves to sodium nitroprusside and acetylcholine in the absence or presence of L-NAME in *mthfr*$^{+/-}$ and wild-type mice

(a) Concentration–response curve to acetylcholine and (b) to sodium nitroprusside (SNP) of noradrenaline-precontracted mesenteric resistance arteries from *mthfr*$^{+/-}$ and wild-type mice. (c) and (d) Concentration–response curve to acetylcholine without or with the NOS inhibitor L-NAME. *$P < 0.05$ compared with HCD (a), and with the concentration–response to acetylcholine (c).

inhibition of mechanisms that contribute to the progression of atherosclerosis [1,28]. TZDs may induce anti-atherogenic effects via different mechanisms, including the normalization of total plasma cholesterol, as shown in rats fed HCD [29] or via direct anti-inflammatory, anti-oxidant and antihypertrophic effects [1,30–32], which may be independent of their metabolic actions. As expected [14], rosiglitazone reduced the lipid deposition found in the aorta of *mthfr*$^{+/-}$ mice (results not shown), potentially via reduction of plasma cholesterol in the mice fed HCD. Inflammatory markers such as VCAM-1 and osteopontin, which were increased in *mthfr*$^{+/-}$ mice, were only slightly decreased by rosiglitazone (results not shown), suggesting that PPARγ agonism did not have a marked anti-inflammatory effect in this particular model. PPARγ agonists block cell proliferation and enhance apoptosis of vascular smooth muscle cells [33,34], suggesting a role of TZDs in the modulation of vascular remodelling. Growth and migration of vascular smooth muscle cells into the intima is a central step of atherosclerotic plaque formation [35]. Hence, rosiglitazone may reduce atherosclerotic lesions in part by improving the vascular remodelling [36]. Rosiglitazone attenuated intimal hyperplasia after arterial balloon catheter injury in a rat model of diet-induced H-Hcy, which presented a 3-fold increase in proliferation of rat aortic vascular smooth muscle cells [37]. In persons with impaired glucose tolerance and no diabetes and cardiovascular disease, rosiglitazone modestly reduced carotid intima-media thickness [38], suggesting anti-atherogenic effects of PPARγ activation occurring particularly via remodelling of the vascular wall in humans. However, in Type 2 diabetic patients, rosiglitazone had no significant effect on carotid atheroma as assessed by three-dimensional carotid magnetic resonance imaging [39].

Endothelial dysfunction contributes to the development of atherosclerotic lesions and vascular remodelling, and its presence and severity is predictive of adverse outcomes [40]. Several cardiovascular risk factors may

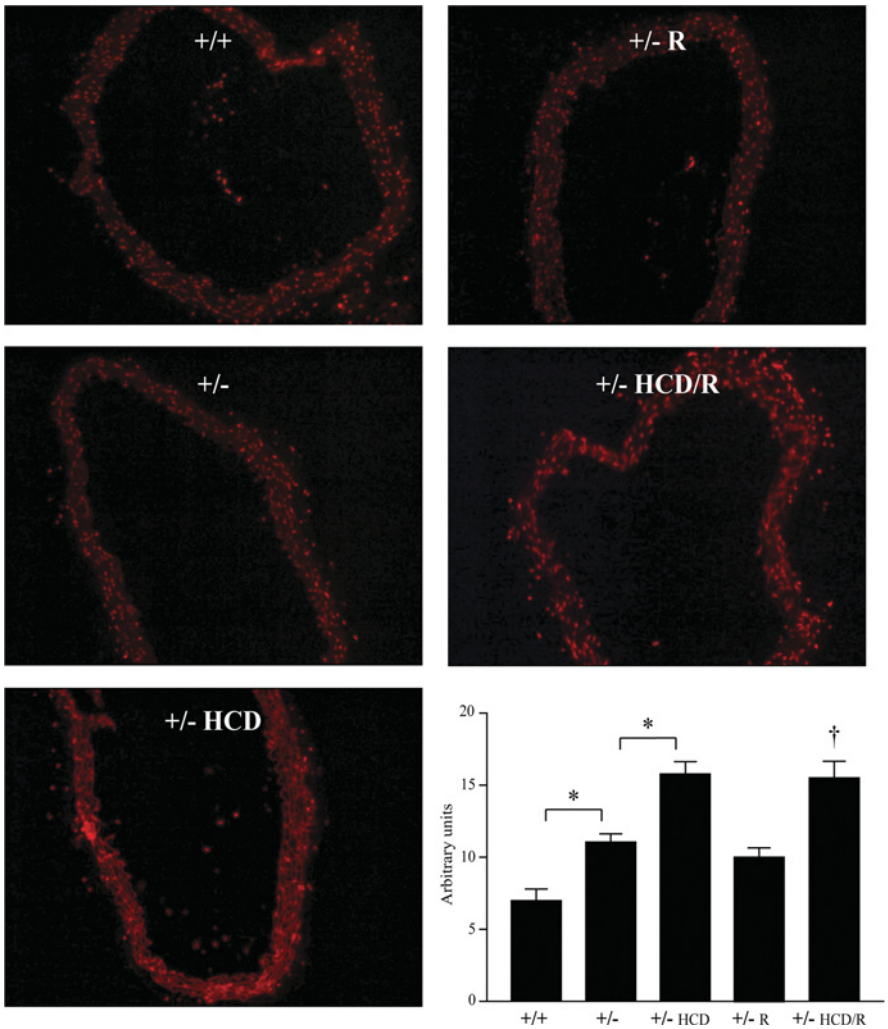

Figure 4 DHE staining of ROS in aorta of *mthfr*$^{+/-}$ and wild-type mice

ROS production was increased in the aorta of *mthfr*$^{+/-}$ mice. *$P < 0.05$; †$P < 0.05$ compared with +/+, +/— and +/— R.

contribute to endothelial dysfunction, including age and hypercholesterolemia, by promoting vascular oxidative stress and impaired NO generation or bioavailability [26,27]. In particular, rabbits fed HCD had reduced NO levels and increased ADMA, an L-arginine analogue that acts as a competitive inhibitor of eNOS [41]. We recently reported that mesenteric arteries of young *mthfr*$^{+/-}$ mice presented endothelial dysfunction due to increased oxidative stress and uncoupling of eNOS [42]. However, the precise mechanisms whereby H-Hcy produces endothelial dysfunction are incompletely defined. Besides decreased NO bioavailability due to increased ROS production, another potential mechanism for reduced NO effects in subjects with H-Hcy is decreased NO production due to increased levels of ADMA [43]. Homocysteine reduces the catabolism and induces the synthesis of ADMA, the latter partially dependent on PRMT-1 activation [44]. Acetylcholine-induced vasodilation of carotid arteries from old *mthfr*$^{+/-}$ mice was similar to that of age-matched wild-type mice and was 30% less then that observed in mesenteric arteries of younger mice [42]. It is possible that increased levels of homocysteine do not induce further impairment of endothelial function in addition to age-related endothelial dysfunction, despite the elevation of ROS levels in aorta of old *mthfr*$^{+/-}$ mice. Rosiglitazone, which reduced oxidative stress in young *mthfr*$^{+/-}$ mice [42], did not reduce increased ROS production in old *mthfr*$^{+/-}$ mice or improve endothelial function in these mice. Rosiglitazone treatment paradoxically resulted in greater impairment of endothelial function in *mthfr*$^{+/-}$ mice fed HCD. It has been recently reported that homocysteine competes for PPAR nuclear receptors with PPAR agonists and may impair the maximum activation of PPAR receptors by the latter. Thus, homocysteine elevation may have an important impact on PPAR agonist

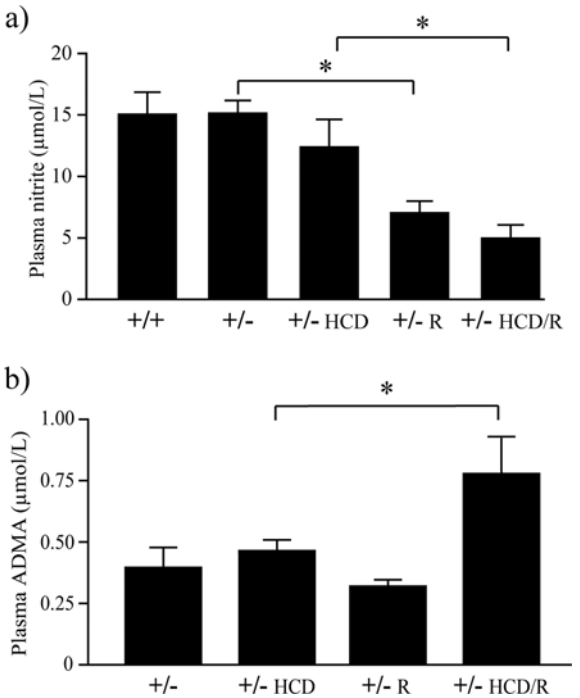

Figure 5 Plasma nitrite in *mthfr*$^{+/-}$ and wild-type mice, and plasma ADMA in *mthfr*$^{+/-}$ mice

(**a**) Plasma nitrite (index of NO production) in *mthfr*$^{+/-}$ and wild-type mice. (**b**) Plasma concentration of the endogenous NOS inhibitor ADMA in *mthfr*$^{+/-}$ mice. *$P < 0.05$.

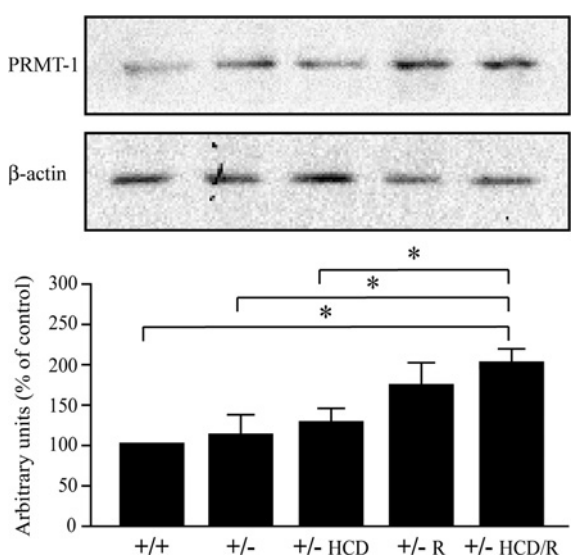

Figure 6 PRMT-1 expression in the aorta of *mthfr*$^{+/-}$ mice

A representative Western blot and corresponding quantification of PRMT-1 levels relative to β-actin are shown. Results are presented as a percentage of PRMT-1 expression in wild-type control mice. *$P < 0.05$.

action [45]. Furthermore, reduced production of NO, plus increased scavenging by excess ROS, may contribute to explaining these results. Indeed, *mthfr*$^{+/-}$ mice fed HCD presented the highest levels of ROS in aorta possibly due to the combined effect of age, high plasma cholesterol and H-Hcy. The endothelial dysfunction of HCD-fed *mthfr*$^{+/-}$ mice treated with rosiglitazone may also explain the absence of improvement of vascular remodelling in this group despite a favourable effect on lipid deposition in atherosclerotic lesions. This suggests a countervailing effect of TZDs on progression of atherosclerosis depending on how many risk factors are contemporaneously present. Interestingly, HCD-fed *mthfr*$^{+/-}$ mice treated with rosiglitazone presented increased expression of PPARγ, which has recently been reported to contribute to rosiglitazone-induced cardiotoxic effects [46].

An intriguing finding was that PRMT-1 was increased in rosiglitazone-treated HCD-fed *mthfr*$^{+/-}$ mice. PRMT-1 is the major source of ADMA in the vasculature [43] and is partially activated by H-Hcy [42,46] as well as by LDL (low-density lipoprotein)-cholesterol [47]. The promoter of *Prmt1* contains PPARγ-responsive elements, which are highly conserved, as shown in Figure 7. Consistent with this finding, ADMA levels were increased approximately 2-fold in rosiglitazone-treated HCD-fed *mthfr*$^{+/-}$ mice. Thus, rosiglitazone via increased expression and therefore activity of PRMT-1 leading to production of ADMA may decrease NO production and promote endothelial dysfunction in HCD-fed old *mthfr*$^{+/-}$ mice, which already present high ROS generation in the vascular wall, thus amplifying this detrimental effect of H-Hcy and HCD.

These observations may support and extend results of recent experimental and clinical studies that challenge the vascular protective role of PPARγ activators in cardiovascular disease. TZDs have adverse effects on advanced atherosclerosis by promoting plaque instability [48], and PPARγ activation may contribute to monocyte differentiation into foam cells [49]. In humans, a recent meta-analysis of rosiglitazone treatment trials in diabetic patients has shown that rosiglitazone may be associated with increased risk of myocardial infarction and death from cardiovascular causes [50], although methodological limitations do not allow definitive conclusions, and this conclusion remains highly controversial. As a result, there is a situation of equipoise regarding the safety of rosiglitazone until further data are obtained [51].

Clinical perspectives

Important new findings from this study are that rosiglitazone may exert beneficial and detrimental effects on the cardiovascular system depending on pre-existing levels of cardiovascular risk. Rosiglitazone exerted vascular protective effects in old mice with H-Hcy by attenuating vascular remodelling as well as the

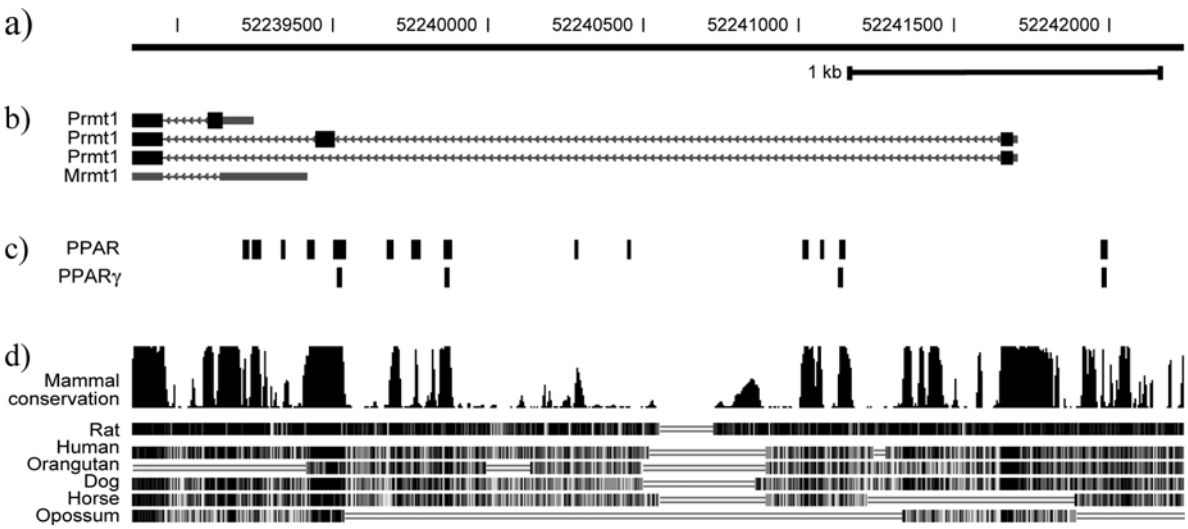

Figure 7 ***In silico*** **analysis of the** ***Prmt1*** **gene**

The 52 238 857–52 242 238 bp region of chromosome 7 (a) containing the two 5′ exons and the promoter region of the *Prmt1* gene responsible for the transcription of four different alternative *Prmt1* mRNA splices (b) are presented. Coding and non-coding exons are indicated by wide black and narrow grey rectangles respectively. Direction of transcription is indicated by arrowheads and is from right to left. (c) Conserved PPAR- and PPARγ-response elements between mouse and human are indicated. (d) Several regions of the *Prmt1* promoter that are highly conserved among mammals are displayed.

atherosclerotic process. However, it was unable to reduce the increased oxidative stress in *mthfr*$^{+/-}$ mice fed or not HCD and exerted minimal effect on inflammatory mediators in these mice. When these mice became hypercholesterolaemic in addition to aging and H-HCy, the prior beneficial effect was counterbalanced by rosiglitazone-induced endothelial dysfunction, which may contribute to cardiovascular remodelling as well as blunting any beneficial effect on atherosclerosis. These findings are consistent with current evidence for a role of PPARγ at the interface between the environment and control of metabolism [52]. Indeed, a common genetic variant of PPARγ in humans induces opposing effects on lipid and glucose metabolism depending on whether individuals are obese or sedentary, and depending on the fat composition of the diet [53]. In conclusion, the present study suggests mechanisms that may explain beneficial effects of PPARγ activation in lower risk subjects, but detrimental actions in the presence of high cardiovascular risk, which could explain some recent clinical observations in diabetic patients with advanced atherosclerosis.

ACKNOWLEDGEMENTS

We thank André Turgeon for his excellent technical work.

FUNDING

This work was supported by the Canadian Institutes of Health Research (CIHR) [grant number 82790], Canada Research Chair (CRC) Program of CIHR/Government of Canada, and the Canada Fund for Innovation (CFI) (all to E.L.S.), and a fellowship from the Heart and Stroke Foundation (to T.E. and C.A.L.).

REFERENCES

1 Touyz, R. and Schiffrin, E. L. (2006) Peroxisome proliferator-activated receptors in vascular biology-molecular mechanisms and clinical implications. Vasc. Pharmacol. **45**, 19–28
2 Tontonoz, P., Hu, E. and Spiegelman, B. M. (1994) Stimulation of adipogenesis in fibroblasts by PPARγ, a lipid-activated transcription factor. Cell **79**, 1147–1156
3 Olefsky, J. M. and Saltiel, A. R. (2000) PPARγ and the treatment of insulin resistance. Trends Endocrinol. Metab. **11**, 362–368
4 Duan, S. Z., Usher, M. G. and Mortensen, R. M. (2008) Peroxisome proliferators-activated receptor-γ-mediated effects in the vasculature. Circ. Res. **102**, 283–294
5 Evans, R. M., Barish, G. D. and Wang, Y. X. (2004) PPARs and the complex journey to obesity. Nat. Med. **10**, 355–361
6 Tontonoz, P., Nagy, L., Alvarez, J. G., Thomazy, V. A. and Evans, R. M. (1998) PPARγ promotes monocyte/macrophage differentiation and uptake of oxidized LDL. Cell **93**, 241–252
7 Marx, N., Sukhova, G. M., Murphy, C., Libby, P. and Plutzky, J. (1998) Macrophages in human atheroma contain PPARγ: differentiation-dependent PPARγ expression and reduction of MMP-9 activity through PPARγ activation in mononuclear phagocytes *in vitro*. Am. J. Pathol. **153**, 17–23
8 Ricote, M., Huang, J., Fajas, L., Li, A., Welch, J., Najib, J., Witztum, J. L., Auwerx, J., Palinski, W. and Glass, C. K. (1998) Expression of the peroxisome proliferator-activated receptor γ (PPARγ) in human atherosclerosis and regulation in macrophages by colony stimulating factors and oxidized low density lipoprotein. Proc. Natl. Acad. Sci. U.S.A. **95**, 7614–7619

9 Staels, B., Koenig, W., Habib, A., Merval, R., Lebret, M., Pineda-Torra, I., Delerive, P., Fadel, A., Chinetti, G., Fruchart, J. C. et al. (1998) Activation of human aortic smooth-muscle cells is inhibited by PPARα but not by PPARγ activators. Nature **393**, 790–793
10 Chinetti, G., Gbaguidi, G. F., Griglio, S., Mallat, Z., Antonucci, M., Poulain, P., Chapman, J., Fruchart, J. C., Tedgui, A., Najib-Fruchart, J. and Staels, B. (2000) CLA-1/SR-BI is expressed in atherosclerotic lesion macrophages and regulated by activators of peroxisome proliferator-activated receptors. Circulation **10**, 2411–2417
11 Robinson, J. G. (2008) Should we use PPAR agonists to reduce cardiovascular risk? PPAR Res, **28**, 891425
12 Welch, G. N. and Loscalzo, J. (1998) Homocysteine and atherothrombosis. N. Engl. J. Med. **338**, 1042–1050
13 Eikelboom, J. W., Lonn, E., Genest, J., Jr, Hankey, G. and Yusuf, S. (1999) Homocysteine and cardiovascular disease: a critical review of the epidemiologic evidence. Ann. Intern. Med. **131**, 363–375
14 Chen, Z., Karaplis, A. C., Ackerman, S. L., Pogribny, I. P., Melnyk, S., Lussier-Cacan, S., Chen, M. F., Pai, A., John, S. W., Smith, R. S. et al. (2001) Mice deficient in methylenetetrahydrofolate reductase exhibit hyperhomocysteinemia and decreased methylation capacity, with neuropathology and aortic lipid deposition. Hum. Mol. Genet. **10**, 433–443
15 Kang, S. S., Zhou, J., Wong, P. W., Kowalisyn, J. and Strokosch, G. (1998) Intermediate homocysteine: a thermolabile variant of methylenetetrahydrofolate reductase. Am. J. Hum. Genet. **43**, 414–421
16 Frosst, P., Blom, H. J., Milos, R., Goyette, P., Sheppard, C. A., Matthews, R. G., Boers, G. J., van den Heijer, M., Kluijtmas, L. A. and van den Heuvel, L. P. (1995) A candidate genetic risk factor for vascular diseas: a common mutation in methylenetetrahydrofolate reductase. Nat. Gen. **10**, 111–113
17 Neves, M. F., Endemann, D., Amiri, F., Virdis, A., Pu, Q., Rozen, R. and Schiffrin, E. L. (2004) Small artery mechanics in hyperhomocysteinemic mice: effects of angiotensin II. J. Hypertens. **22**, 959–966
18 Javeshghani, D., Sairam, R. M., Schiffrin, E. L. and Touyz, R. M. (2007) Increased blood pressure, vascular inflammation, and endothelial dysfunction in androgen-deficient follitropin receptor knockout male mice. J. Am. Soc. Hyper. **1**, 353–361
19 Rothe, G. and Valet, G. (1990) Flow cytometric analysis of respiratory burst activity in phagocytes with hydroethidine and 2′,7′-dichlorofluorescein. J. Leukocyte Biol. **47**, 440–448
20 Miller, F. J. Jr., Gutterman, D. D., Rios, C. D., Heistad, D. D. and Davidson, B. L. (1998) Superoxide production in vascular smooth muscle contributes to oxidative stress and impaired relaxation in atherosclerosis. Circ. Res. **82**, 1298–1305
21 Savoia, C., Ebrahimian, T., He, Y., Gratton, J. P., Schiffrin, E. L. and Touyz, R. M. (2006) Angiotensin II/AT2 receptor-induced vasodilation in stroke-prone spontaneously hypertensive rats involves nitric oxide and cGMP-dependent protein kinase. J. Hypertens. **24**, 2417–2422
22 Kent, W. J., Sugnet, C. W., Furey, T. S., Roskin, K. M., Pringle, T. H., Zahler, A. M. and Haussler, D. (2002) The human genome browser at UCSC, Genome. Res. **12**(6), 996–1006
23 Reference deleted
24 Loots, G., Ovcharenko, I., Pachter, L., Dubchak, I. and Rubin, E. (2002) rVISTA for comparative sequence-based discovery of functional transcription factor binding sites. Genome. Res. **12**, 832–839
25 Reference deleted
26 Savoia, C. and Schiffrin, E. L. (2006) Inhibition of the renin angiotensin system: implications for the endothelium. Curr. Diabetes Rep. **6**, 274–278
27 Touyz, R. and Schiffrin, E. L. (2004) Reactive oxygen species in vascular biology: implications in hypertension. Histochem. Cell. Biol. **122**, 339–352
28 Heikkinen, S., Auwerx, J. and Argmann, C. A. (2007) PPARγ in human and mouse physiology. Biochim. Biophys. Acta **1771**, 999–1013
29 Schaalan, M., El-Abhar, S., Maged, B. and El-Deshary, E. S. (2009) Westernized-like-diet-fed rats: effect on glucose homeostasis, lipid profile, and adipocyte hormones and their modulation by rosiglitazone and glimepiride. J. Diabetes Complicat. **23**, 199–208
30 Li, A. C., Brown, K. K., Silvestre, M. J., Wilson, T. M., Palinski, W. and Glass, C. K. (2000) Peroxisome proliferator-activated receptor γ ligands inhibit development of atherosclerosis in LDL-receptor knock-out mice. J. Clin. Invest. **106**, 523–531
31 Minamikawa, J., Tanaka, S., Yamauchi, M., Inoue, D. and Koshiyama, H. (1998) Potent inhibitory effect of troglitazone on carotid arterial wall thickness in type 2 diabetes. J. Clin. Endocrinol. Metab. **83**, 1818–1820
32 Chen, Z., Ishibashi, S., Perrey, S., Osuga, J., Gotoda, T., Kitamine, T., Tamura, Y, Okazaki, H., Yahagi, N., Iizuka, Y. et al. (2001) Troglitazone inhibits atherosclerosis in apolipoprotein E-20 knock-out mice: pleiotropic effect on CD36 expresion and HDL. Arterioscl. Thromb. Vasc. Biol. **21**, 372–377
33 Marx, N., Schonbeck, U., Lazar, M. A., Libby, P. and Plutzky, J. (1998) Peroxisome proliferator activated receptor γ activators inhibit gene expression and migration in human vascular smooth cells. Circ. Res. **83**, 1097–1103
34 Bruemmer, D., Yin, F., Liu, J., Berger, J. P., Sakai, T., Blaschke, F., Fleck, E., Van Herle, A. J., Forman, B. M. and Law, R. E. (2003) Regulation of the growth arrest and DNA damage inducible gene 45 (GADD45) by peroxisome proliferator-activated receptor γ in vascular smooth muscle cells. Circ. Res. **93**, e38–e47
35 Ross, R. (1999) Atherosclerosis: an inflammatory disease. N. Engl. J. Med. **340**, 115–126
36 Collins, A. R., Meehan, W. P., Kintscher, U., Jackson, S., Wakino, S., Noh, G., Palinski, W., Hsueh, W. A. and Law, R. E. (2001) Troglitazone inhibits formation of early atherosclerotic lesion in diabetic and non diabetic low density lipoprotein receptor deficient mice. Arterioscl. Thromb. Vasc. Biol. **21**, 365–371
37 Murthy, S. N., Obregon, D. F., Chattergoon, N. N., Fonseca, N. A., Mondal, D., Dunne, J. B., Diez, J. G., Jeter, Jr, J. R, Kadowitz, P. J., Agrawal, K. C., McNamara, D. B. and Fonseca, V. A. (2005) Rosiglitazone reduces serum homocysteine levels, smooth muscle proliferation, and intimal hyperplasia in Sprague–Dawley rats fed high methionine diet. Metab. Clin. Expt. **54**, 645–652
38 Lonn, E. M., Gerstein, H. C., Sheridan, P., Smith, S., Diaz, R., Mohan, V., Bosch, J., Yusuf, S. and Dagenais, G. R. (2009) Effect of ramipril and of rosiglitazone on carotid intima-media thickness in people with impaired glucose tolerance or impaired fasting glucose: STARR (STudy of Atherosclerosis with Ramipril and Rosiglitazone). J. Am. Coll. Cardiol. **53**, 2028–2035
39 Varghese, A., Yee, M. S., Chan, C. F., Crowe, L. A., Keenan, N. G., Johnston, D. G. and Pennell, D. J. (2009) Effect of rosiglitazone on progression of atherosclerosis: insights using 3D carotid cardiovascular magnetic resonance. J. Cardiovasc. Magn. Reson. **11**, 24–32
40 Schachinger, V., Britten, M. B. and Zehier, A. M. (2000) Prognostic impact of coronary vasodilator dysfunction on adverse long-term outcome of coronary heart disease. Circulation. **101**, 1899–1906

41 Bolayirli, I. M., Aslam, M., Balci, H., Altug, T., Hacibekiroglu, M. and Seven, A. (2007) Effects of atorvastatin therapy on hypercholesterolemic rabbits with respect to oxidative stress, nitric oxide pathway and homocysteine. Life Sci. **81**, 121–127
42 Virdis, A., Iglarz, M., Neves, M. F., Amiri, F., Touyz, R. M., Rozen, R. and Schiffrin, E. L. (2003) Effect of hyperhomocysteinemia and hypertension on endothelial function in methylene tetrahydrofolate reductase-deficient mice. Arterioscl. Thromb. Vasc. Biol. **23**, 1352–1357
43 Valance, P. and Leiper, J. (2004) Cardiovascular biology of the asymmetric dimethylarginine: dimethylarginine dimethylaminohyddrolase pathway. Arterioscl. Thromb. Vasc. Biol. **24**, 1023–1030
44 Lentz, S. R. and Rodinov, R. N., (2003) Dayal, S. Hyperhomocysteinemia, endothelial dysfunction and cardiovascular risk: the potential role of ADMA. Atherosclerosis **4**, 61–65
45 Hayden, M. R. (2008) Homocysteine competes for the peroxisome proliferator-activated receptor nuclear receptors. J. Cardiometab. Syndr. **3**, 70–71
46 Son, N. H., Park, T. S., Yamashita, H., Yokoyama, M., Huggins, L. A., Okajima, K., Homma, S., Szabolcs, M. J., Huang, L. S. and Goldberg, I. J. (2007) Cardiomyocyte expression of PPARγ leads to cardiac dysfunction in mice. J. Clin. Invest. **117**, 2791–2801
47 Böger, R. H., Sydow, K., Borlak, J., Thum, T., Lenzen, H., Schubert, B., Tsikas, D. and Bode-Böger, S. M. (2000) LDL cholesterol upregulates synthesis of asymmetrical dimethylarginine in human endothelial cells: involvement of *S*-adenosyl methionine-dependent methyltransferases. Circ. Res. **87**, 99–105
48 Thorp, E., Kuriakose, G., Shah, Y. M., Gonzalez, F. J. and Tabas, I. (2007) Pioglitazone increases macrophage apoptosis and claque necrosis in advanced atherosclerotic lesions of non diabetic low-density lipoprotein receptor-null mice. Circulation **116**, 2182–2190
49 Tontonoz, P., Nagy, L., Alvarez, J. G., Thomazy, V. A. and Evans, R. M. (1998) PPAR γ promotes monocyte/macrophage differentiation and uptake of oxidized LDL. Cell **93**, 241–252
50 Nissen, S. E. and Wolski, K. (2007) Effect of rosiglitazone on the risk of myocardial infarction and death from cardiovascular causes. N. Engl. J. Med. **356**, 2457–2471
51 Psaty, B. M. and Furberg, C. D. (2007) Rosiglitazone and cardiovascular risk. N. Engl. J. Med. **356**, 522–2524
52 Semple, R. K., Chatterjee, V. K. and O'Rahilly, S. (2006) PPAR γ and human metabolic disease. J. Clin. Invest. **116**, 581–589
53 Luan, J., Brawne, P. O., Harding, A. H., Halsall, D. J., O'Rahilly, S., Chatterjee, V. K. and Wareham, N. J. (2001) Evidence of gene-nutrient interaction at the PPAR γ locus. Diabetes **50**, 686–689

Received 27 May 2009/25 November 2009; accepted 1 December 2009
Published as Immediate Publication 1 December 2009, doi:10.1042/CS20090289